J. Fluid Mech. (1971), *vol.* 46, *part* 1, *pp.* 43–64
Printed in Great Britain

An experimental investigation of pulsating turbulent water flow in a tube

By J. H. GERRARD
Department of the Mechanics of Fluids, University of Manchester

(Received 27 April 1970)

Experiments were made on a pulsating water flow at a mean flow Reynolds number of 3770 in a cylindrical tube of diameter 3·81 cm. Pulsations were produced by a piston oscillating in simple harmonic motion with a period of 12 s. Turbulence was made visible by means of a sheet of dye produced by electrolysis from a fine wire stretched across a diameter. The sheet of dye is contorted by the turbulent eddies, and ciné-photography was used to find the velocity of convection which was shown to be the flow speed except in certain circumstances which are discussed. By subtracting the mean flow velocity profile the profile of the component of the motion oscillating at the imposed frequency was determined.

The Reynolds number of these experiments lies in the turbulent transition range, so that large effects of laminarization are observed. In the turbulent phase, the velocity profile was found to possess a central plateau as does the laminar oscillating profile. The level and radial extent of this were little different from the laminar ones. Near to the wall, the turbulent oscillating profile is well represented by the mean velocity power law relationship, $u/U \propto (y/a)^{1/n}$. In the laminarized phase, the turbulent intensity is considerably reduced at this Reynolds number. The velocity profile for the whole flow (mean plus oscillating) relaxes towards the laminar profile. Laminarization contributes appreciably to the oscillating component.

Extrapolation of the results to higher Reynolds numbers and different frequencies of oscillation is suggested.

1. Introduction

The laminar pulsating flow in a cylindrical pipe away from the region affected by the ends was determined analytically by Sexl (1930) and by Szymanski (1930). Other treatments have been published by Womersley (1955), Uchida (1956) and others. Corroborative measurements of the oscillating velocity profile have been made by Linford & Ryan (1965). To study the corresponding problem in a turbulent flow is considerably more difficult experimentally and impossible analytically. The complication is increased not only because the flow is turbulent, but also by the fact that the turbulent intensity varies through the cycle of oscillation, all the more so when the amplitude of oscillation is large enough to produce an appreciable effect on the velocity profile. Some measurements on pulsating turbulent pipe flow have been made, for example by Combs (1964), but nowhere

does there seem to have been reported any work on the detail of the velocity profile after the manner of Linford and Ryan in laminar flow.

The design of an experiment to study pulsating pipe flow is something of a compromise. The three parameters which govern laminar pulsating pipe-flow of incompressible fluid are inter-related, and have also to be matched to reasonable values of size of apparatus, frequency of oscillation and the choice of working fluid. These principal parameters are the mean flow Reynolds number Re, the non-dimensional frequency Ω, and the non-dimensional amplitude of oscillation λ, where

U = time average of the sectional mean velocity,
a = pipe radius,
ν = coefficient of kinematic viscosity,
ω = angular frequency of the simple harmonic oscillation,
x_0 = amplitude of the piston producing the oscillation,
$Re = 2Ua/\nu$,
$\Omega = a\sqrt{(\omega/\nu)}$,
and $\lambda = \omega x_0/U$.

The frequency parameter Ω is a measure of the ratio of the tube radius to the distance through which vorticity produced at the wall will diffuse in one period of the oscillation.

Re	3770	$2\pi/\omega$	12·185 s
Ω	14·40	a	1·90 cm
λ	0·573	x_0	9·9 cm
U	8·91 cm s^{-1}	Camera frame speed	24 s^{-1}

TABLE 1. Values of the main parameters adopted for pulsating water flow

It was decided to use water as the fluid, and to measure velocity by marking the fluid and taking photographs. The requirements for this particular experiment are (i) that the flow shall be turbulent, which fixes a lower limit to Re, (ii) that the frequency shall be high enough to produce a pulsating boundary layer which must not be so thin that it is lost in a thin layer near the wall (this fixes a range of Ω), and (iii) that the amplitude must be such that the oscillations in velocity are not small compared with the mean flow speed U. Significant reversed flow must not be produced because this complicates interpretation of the results. Other considerations also enter. A ciné camera with maximum speed of 64 frames per second was available and the framing period must be a small fraction ($\leqslant \frac{1}{360}$) of the period of oscillation of the flow. A consideration of these mutually interfering requirements, together with a stipulation that the reciprocating arrangement must not be too large, confines all the independent variables within fairly narrow limits. The final choice of values is listed in table 1.

At this Reynolds number there is a high degree of laminarization; the turbulent structure of the flow almost disappears for about half the cycle of oscillation.

A higher Reynolds number could not be obtained without a pulsator which could only be classed as heavy machinery. The effect of laminarization is not as great as might at first sight be supposed. It has been successfully accounted for in the discussion of results, and a generalization from the present results to higher Reynolds numbers is possible.

An introduction to the method of the experiment and the form of the flow is best obtained by reference to figures 1–3 (plates 1–5), which show the appearance of a dyed sheet of water at various times throughout the cycle of oscillation. A fuller description will follow in later sections. Each plate shows at the top a view vertically downward on to the transparent pipe and below the horizontal view through a mirror. Figure 1 shows the calibration grid with rulings at 5 and 10 mm spacing. On the other photographs there is flow from left to right. At the extreme left of the figures is the fine dye-producing wire. The sheet of dye can be seen with striations due to dirt and bubbles attached to the wire. The turbulent eddies fold the sheet of dye. It thus appears darker where the plane of the dye is in the line of sight. Figure 2 shows the steady turbulent flow at the same mean velocity as in the pulsating flow which follows in figures 3 to 10. These were taken at approximately equal intervals through the cycle with a separation of $\frac{1}{8}$ cycle. $\omega t = 0$ corresponds to the piston fully retracted. The variation of the turbulence intensity through the cycle is immediately apparent. The wires crossing the tube at the top of each photograph reciprocate with the piston and serve to mark its position on the photograph.

In view of the extremely lengthy process of reduction of the results by the method adopted here, the oscillating velocity profiles were measured at only two times during the cycle. These two times were chosen on the basis of the laminar flow profiles derived in the manner of § 2.

2. Oscillating component of the velocity in laminar flow

By a consideration of the theory for laminar oscillating flow it will be shown that far from the oscillating piston the velocity profiles are the same as those in an infinite tube to which an oscillating pressure gradient is applied. The establishment distance will depend on the Reynolds number of the mean flow, the amplitude of oscillation λ and the frequency Ω. The establishment length will oscillate during the cycle being longest at the highest speed when the piston is moving at maximum speed in the direction of the mean flow. At the lowest frequencies one expects the mean establishment length to be about the same as the entrance length for steady flow in the pipe. At the mean Reynolds number of these experiments this is 120 diameter or 4·6 m. At high frequency a central core of the flow moves with the piston and the thickness we are concerned with for the establishment of the flow is the oscillating boundary-layer thickness rather than the tube radius. At the frequency of this experiment the boundary-layer thickness is approximately half the tube radius (see figure 4(*a*)), and so the mean entrance length is about 2·3 m. The measuring position is at 3·6 m along the straight section of the pipe and 2·8 m from the piston. We conclude that the tube is just long enough if we confine our measurements to the parts of the cycle where the

establishment length has its mean value or less. Measurements were made at $\omega t = 0$ and $\frac{1}{2}\pi$.

The velocity distribution and its time variation may be abstracted from Uchida's (1956) analytical solution for laminar pulsations in an infinite cylindrical pipe of circular cross-section. The sectional mean velocity is simply equated to the piston speed.

The equation of motion relating velocity u and pressure p to time t, axial distance x and radial distance r is

$$\frac{\partial u}{\partial t} = \frac{-1}{\rho}\frac{\partial p}{\partial x} + \nu\left(\frac{\partial^2 u}{\partial r^2} + \frac{1}{r}\frac{\partial u}{\partial r}\right). \tag{1}$$

Consider only the oscillating component of the motion, which is to be simply added to the (laminar) mean flow. Following Uchida (1956), let the oscillating part of the pressure gradient be given by

$$\frac{-1}{\rho}\frac{\partial p}{\partial x} = \kappa \cos nt. \tag{2}$$

The solution of (1) is in this case

$$u = \frac{\kappa}{\mu k^2}\{B\cos nt + (1-A)\sin nt\}, \tag{3}$$

where

$$\left.\begin{aligned} k &= \sqrt{(n/\nu)}, \\ A &= \frac{\operatorname{ber} ka \operatorname{ber} kr + \operatorname{bei} ka \operatorname{bei} kr}{\operatorname{ber}^2 ka + \operatorname{bei}^2 ka}, \end{aligned}\right\} \tag{4}$$

and

$$\left. B = \frac{\operatorname{bei} ka \operatorname{ber} kr - \operatorname{ber} ka \operatorname{bei} kr}{\operatorname{ber}^2 ka + \operatorname{bei}^2 ka}. \right\}$$

ν is the coefficient of kinematic viscosity and a is the radius of the tube. By integrating over the cross-section the sectional mean velocity u_m is obtained

$$u_m = \frac{\kappa}{\mu k^2}\left\{\frac{2D}{ka}\cos nt + \left(1 - \frac{2C}{ka}\right)\sin nt\right\}, \tag{5}$$

$$= \frac{\kappa}{\mu k^2}\sigma \cos(nt - \delta), \tag{6}$$

where

$$\left.\begin{aligned} C &= \frac{\operatorname{ber} ka \operatorname{bei}' ka - \operatorname{bei} ka \operatorname{ber}' ka}{\operatorname{ber}^2 ka + \operatorname{bei}^2 ka}, \\ D &= \frac{\operatorname{ber} ka \operatorname{ber}' ka + \operatorname{bei} ka \operatorname{bei}' ka}{\operatorname{ber}^2 ka + \operatorname{bei}^2 ka}, \\ \sigma^2 &= \left(1 - \frac{2C}{ka}\right)^2 + \left(\frac{2D}{ka}\right)^2, \\ \tan\delta &= (1 - 2C/ka)/(2D/ka). \end{aligned}\right\} \tag{7}$$

Let the piston position be

$$x = x_0 \cos \omega t. \tag{8}$$

The piston speed is the mean flow speed, therefore,

$$u_m = \dot{x} = -\omega x_0 \sin \omega t$$
$$= \omega x_0 \cos(\omega t - \tfrac{1}{2}\pi). \tag{9}$$

Comparison with (6) gives

$$\frac{\kappa\sigma}{\mu k^2} = \omega x_0 \quad \text{and} \quad nt - \delta = \omega t - \tfrac{1}{2}\pi. \tag{10}$$

The expression for the oscillating component of the velocity is thus

$$u = \omega x_0 \frac{\sigma_1}{\sigma} \cos(\omega t - \tfrac{1}{2}\pi + \delta - \phi), \tag{11}$$

where $$\sigma_1^2 = (1-A)^2 + B^2,$$

and $$\tan\phi = (1-A)/B.$$

Velocities calculated from (11) are plotted in figure 4. The velocity values are for a piston speed given by (11) with $\omega x_0 = 5{\cdot}10$ cm/s which corresponds to the values in table 1. Figure 4 (*a*) shows velocity profiles during half the cycle. Measurements were made at $\omega t = 0$ and $\frac{1}{2}\pi$; at these two times in the piston cycle the effect of variation of frequency Ω on the velocity profile is shown in figure 4 (*b*) and (*c*).

A physical description of the ways in which the laminar oscillating profile arises will be of assistance when in § 7 we discuss the profiles in turbulent flow. Consider the flow far from the piston and from other end effects. In laminar flow in a long tube the flow is parallel to the axis and so independent of distance along the tube. In parallel laminar flow the non-linear terms are absent from the equations of motion. Linearity implies that the mean and oscillating components of the flow are decoupled and thus we may consider the oscillating component alone. As the piston oscillates the velocity profile changes as a result of two effects. Vorticity created only at the wall diffuses into the flow. In this flow the vorticity is simply the radial gradient of velocity. This diffusion is the progress in time towards the laminar steady flow parabolic profile, but there exists a constantly changing situation. The relevant parameter is therefore Ω which is a measure of the ratio of the tube radius to the distance vorticity diffuses in one period of oscillation. Apart from considerations of stability of the flow at high Reynolds number, the Reynolds number does not enter as a relevant parameter. The viscosity ν entering into $a^2/\nu t$ simply determines the time scale. At high frequency there exists in the centre of the pipe a region of uniform speed into which vorticity never has time to diffuse before being annulled by oppositely signed vorticity. The other effect, which changes the velocity over the whole cross-section, is that of the continuity condition, by which the sectional mean velocity must equal the piston speed at each instant. Retardation due to viscous effects near the wall is balanced by an acceleration over the rest of the cross section. At high frequency Ω viscous effects are confined to a thin oscillating boundary layer and the central core moves like a plug. The phase difference between the piston and the central flow decreases as the frequency increases. At low frequency the profile is that of the steady flow corresponding to the instantaneous value of the mean velocity.

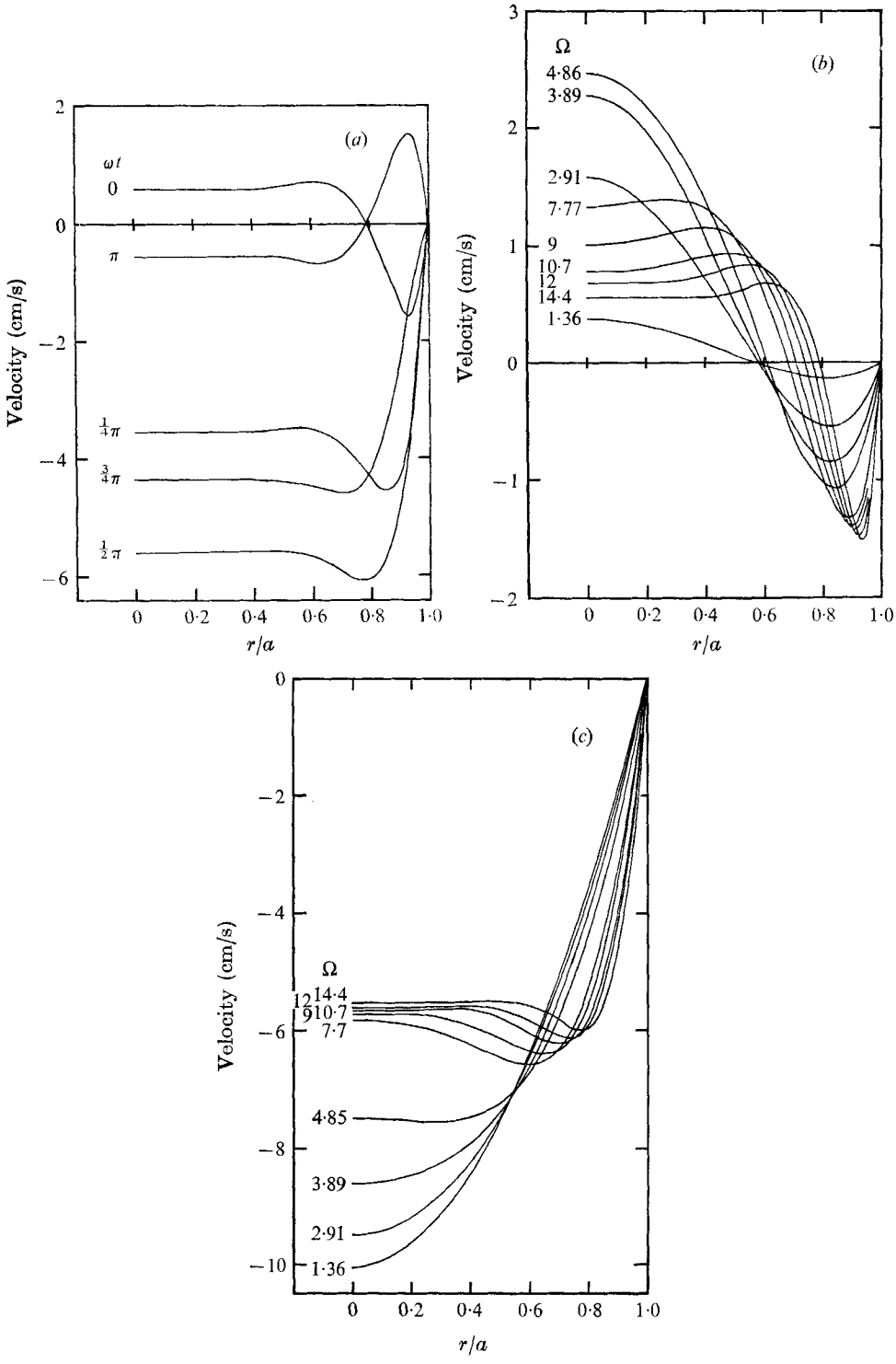

FIGURE 4. Oscillating velocity profiles in laminar flow. Velocity as a function of (*a*) time, (*b*) non-dimensional frequency at $\omega t = 0$, and (*c*) the same at $\frac{1}{2}\pi$.

3. Apparatus

The pulsating pipe flow system is shown in figure 5. Water flows from a constant head device H, through a tube of 3·8 cm internal diameter. In the outlet manifold M, the water escapes through eight holes of 0·16 cm diameter into an annular space, and thence via outlet tubing of 1·27 cm diameter to various outlet constrictions, which may be chosen by the use of valves. The outlet used in these experiments, which were performed at the highest speed of the system, was full bore of

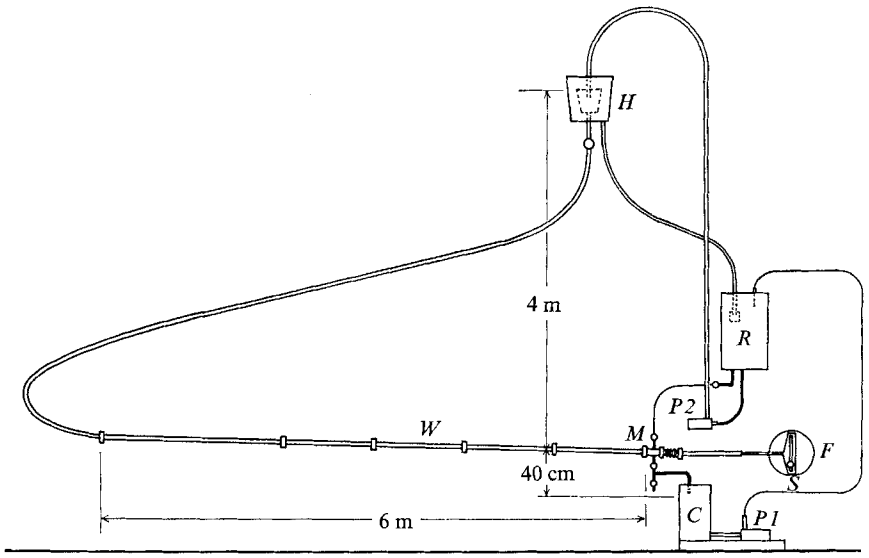

FIGURE 5. Schematic of pulsating water-flow apparatus. ═══, diameter 3·8 cm; ═══ 1·27 cm; ——, 1 cm.

the 1·27 cm diameter tubing. The water discharges into the collecting tank C, which is used as a measuring station. The tank is equipped with an automatic float switch to discharge the fluid by means of pump P 1 when the water surface is above a predetermined level and rising. The pump switches off when the surface is below a lower level. The water is stored in the main reservoir R. Pump P 2, is capable of delivering 76 ml./s to the constant head device. This rate of flow is seven times the maximum flow rate through the working section. The overflow is returned to the reservoir R. The excessive rate of pumping raises the temperature of the water by a few degrees after an hour's running. Thermal effects were not found to be troublesome in these experiments.

The main tube extends beyond the outlet manifold through a flexible joint to a cylinder of the same diameter in which a piston may be reciprocated in simple harmonic motion by the Scotch Yoke arrangement S. The flywheel F is driven by a $\frac{1}{4}$ h.p. electric motor through gear boxes and a continuously variable 'Kopp variator'. By this means the flywheel frequency can be adjusted within the range of approximately 0·1–0·01 Hz.

At the low Reynolds numbers for which the apparatus was intended the pipe entrance in the constant head tank need not be smooth. It contains a four-vane splitter to inhibit swirl: other disturbances die out in the 8 m length of flexible tubing between the inlet and the first flange of the straight pipe system. Entry disturbances are largely responsible for transition to turbulence in pipe flow and thus the rough entry ensures that at the relatively low Reynolds number of the present experiments the pipe flow shall be turbulent. The flexible tubing (P.V.C. flexilant hose) is reinforced plastic which maintains its circular cross-section when bent. The first 2 m of the straight pipe is commercial brass tubing of nominal 3·82 cm bore. The following four sections each 1 m in length are interchangeable and in these experiments were brass, Perspex, Perspex, and brass, respectively. The brass tubes are waveguide tubing of internal diameter $3{\cdot}810 \pm 0{\cdot}004$ cm. The Perspex tubes are selected tubing of almost the same diameter. Their diameter varies and also their cross-section by as much as $\pm$ 0·03 cm. These tubes were bored circularly cylindrical at the ends to a diameter of 3·830 cm. The tubes carry plane flanges and are joined by adaptor pieces carrying rubber *O*-rings. The internal diameter of the adaptors is $3{\cdot}820 \pm 0{\cdot}005$ cm and they are about 1·5 cm long. In this way steps at the tube joints were minimized. The piston cylinder was also waveguide tubing. The piston was sealed with a rubber *O*-ring.

The straight tube was inclined at an angle of $\tan^{-1} \frac{1}{36}$ to the horizontal to prevent bubbles lodging in the tube. The lower part of the system was filled from the reservoir by slow gravity feed in order to avoid the production of bubbles which would follow the first surge of water from the upper tank when the pump was switched on.

The principle of operation of the system depends upon the outlet tube and constriction presenting a considerably greater flow impedance than the main tube. When this condition is fulfilled the oscillation produced by the piston passes up the working section and not into the outlet. In the present experiment this impedance ratio is at its least effective, but even here the steady turbulent flow pressure drop in the main tube is only 10^{-3} of the pressure drop across the outlet. No pulsations in the outlet flow were evident. The pressure fluctuation due to the piston oscillation is about 10^{-4} times the pressure drop across the outlet, and so it is not surprising that no outlet pulsations are observed.

The mean velocity was determined from the measured rate of volume flow. Water was collected at the outlet in a measuring cylinder. This measurement was accurate to better than 1 % at the high rates of flow used (*ca.* 100 ml./s). The volume flow is temperature sensitive and so the volume flow was determined immediately before and after measurements were made in the working section.

4. Techniques of velocity measurement

Velocity was measured by means of photography of the motion of marked fluid in the working section (at *W* in figure 5). The technique has been described by Baker (1966), and involves the addition of thymol blue to the water to indicate

the change in pH value in the wake of a fine wire electrode. A platinum wire of 25 μm diameter was stretched across the flow tube and made the cathode. The anode was the adjacent brass tube 30 cm from the wire. Electrolysis produces hydrogen at the cathode. If the voltage is low the hydrogen is produced slowly enough to dissolve rather than form bubbles. As hydrogen ions combine to form molecules and give up their charge to the electrode, the water at the cathode possesses an excess of hydroxyl ions and is thus alkaline. The colour change from orange to dark blue takes place at a pH of 8 to 9·6. Caustic soda solution is therefore added to the solution in sufficient quantity to bring it to the verge of its end-point. The life of the solution was found not to be very long when tap water was used, presumably due to organic constituents acting on the thymol blue. Distilled water (40 l.) was therefore used. This solution is found to be still usable after 18 months, though an orange precipitate which develops needs filtering out. Some filtration is included at the end of the overflow return line, but this became inadequate. In order to increase the intensity of the dye a small quantity of common salt (0·03 g/l.) was added to the solution to increase the conductivity. It is possible that the salt increases the precipitation. The visibility of the dye decreases as the flow speed increases; hence the efforts to increase dye intensity. In order to make the dye clearly visible a high potential difference was applied between the electrodes and consequently some hydrogen bubbles were produced. The buoyancy of the marker is seen from figures 2 and 3 (plates 1–5) not to have any appreciable effect. By pulsing the voltage applied to the wire, bands of dye can be produced. These have clearly defined edges at low flow speeds, but at higher speeds the edges become diffuse. In turbulent flow therefore a continuous voltage was applied. The turbulent motions distort the sheet of dye and those convolutions which turn the sheet towards the observer appear darker. The speed of convection of these dark regions may be measured if their shape does not alter significantly in the measuring interval. The speed of convection is the local flow speed except in regions of high radial gradient of velocity. This effect will be discussed below. Ciné films were taken at 24 frames/s; in these the framing interval corresponds to about 4 mm travel at the mean flow speed.

The contrast between the orange-yellow liquid and the dyed liquid which is blue is greatest in yellow light. The flow was observed against the bright background of a paper screen illuminated from behind with a 140 W sodium discharge lamp. The camera was arranged to look directly perpendicularly to the plane of dye and through a mirror along the plane of the dye.

It is known that there is an appreciable error in this method of velocity measurement due to the dye being in the reduced velocity wake of the wire. Davis & Fox (1967) have investigated this effect in laminar flow for the hydrogen bubble technique. The wake velocity deficit should diminish as $x^{-\frac{1}{2}}$, where x is distance downstream from the wire, in laminar or turbulent uniform flow (see Schlichting 1955). Our preliminary measurements in laminar flow showed an $x^{-\frac{1}{2}}$ variation, in contrast to the $x^{-\frac{1}{3}}$ found by Davis & Fox. As we shall see below, the measurements in a turbulent flow generally reach the asymptotic value much more quickly, and so the law which the velocity deficity follows was not determined.

5. Method of measurement

In order to determine the velocity of dye patches, it is necessary to calibrate the field of view. An engraved scale was inserted into the tube. The scale was machined, so that, when placed in the tube, its top surface lay in the meridional plane coinciding with the central plane of the wake of the wire. The scale scribed at 5 and 10 mm spacing was checked on a measuring machine. A photograph of the scale in the liquid filled tube, as seen in figure 1, was taken with the ciné camera before and after the dye visualized turbulent flows.

Velocity was measured from the ciné film of the flowing dye. The images were projected on to a screen with a magnification of about six. The calibration grid photograph was projected on to a white card and the cross-over points of the graticule marked on the card as well as fiducial marks which enabled exact superposition of a dye photograph. Steady turbulent flow velocities were measured first in order to test the method. Inspection of the projected film showed patches of dye which convected with little change of shape. A sheet of tracing paper was fixed over the white card and the outlines of dye patches were drawn in from consecutive frames. The relevant grid points were traced from the white card also. Tracing in coloured pencil distinguished the outline from different frames. The tracings thus contained dye position and increments of time and so velocity could be determined. The frame speed of the camera was found from films of a stop watch taken before and after the turbulence photographs. The camera was found to achieve its synchronous speed in less than 10 frames and thereafter the speed remained constant.

The same procedure was followed for pulsating flow with the addition that the phase of the piston motion was included in the photograph. A pair of fine wires attached to the yoke passed along the top of the tube and were secured at the other end of the tube by means of rubber bands which kept the wires taut for all positions of the piston. Wires with distinguishing marks were attached across the reciprocating wires and these moved across the field of view. The cross-wires which moved just above the tube surface can be seen in figures 2 and 3 (plates 1–5).

Film was taken around two values of the piston position: $\omega t = 0$, corresponding to the piston fully retracted, and $\omega t = \frac{1}{2}\pi$, corresponding to the maximum velocity in the upstream direction. One frame on the film corresponded to about one degree of arc of the piston cycle. Ten frames on either side of the two piston positions were used for measuring flow speeds. At $\omega t = 0$ a significant velocity change occurs over this range of angle. Laminar pulsating flow profiles calculated in this region showed that the variation in velocity was $0{\cdot}1 \pm 0{\cdot}01$ cm/s per degree of arc over the whole cross-section except very close to the wall. A correction was applied on the basis of this to the measured drift distance in one frame interval. At $\omega t = \frac{1}{2}\pi$ the rate of velocity change is an order of magnitude smaller than at $\omega t = 0$ and was neglected.

6. Reduction of results

Measurement of velocity by the method described is subject to error. The errors introduced are mainly due to tracing the outline of a somewhat diffuse patch of dye. These errors are random. A reduction in the spread of the measurements is possible by using a more refined method of measurement such as measuring the negatives with a measuring machine. The results still need statistical treatment and thus little would be gained for a great increase of labour. The measured drift distances Δx during one camera framing interval were grouped into ranges of radial position and of axial distance downstream of the generating wire. The axial ranges were 2 cm long, the radial ranges 0·1 or 0·2 radii depending on the radial gradient of velocity. Each group was accumulated until a reasonable distribution curve was produced. This required 30 to 40 points or more in each group. The readings possess a distribution not only because of error but also by virtue of the true turbulent fluctuation in the measured drift. The r.m.s. deviation in steady turbulent flow was compared with Sandborn's (1955) turbulent intensity results. The effective turbulence in this experiment was 2 to 3 times the true value, though it did show an increase from axis to wall of the tube in the same way that the true turbulence intensity does.

The closeness of the distributions to Gaussian can be seen in figure 6 which shows the measured and Gaussian distributions for one radial position over the range of distances downstream from the dye-producing wire. For each group the mean value was determined and at $\omega t = \frac{1}{2}\pi$ the error of the mean. The latter was found not to be needed, and so was not determined for $\omega t = 0$. The mean values were plotted as a function of distance downstream from the wire. The result at the two phase angles is shown in figures 7 and 8. The numbers by the side of the points indicates the number of measurements involved in determining the mean. The errors of the means is indicated in figure 7.

The values of the radial positions shown in these figures are the ranges measured directly from the plan view of the dye. Examination of the side view in figures 2 and 3 (plates 1–5) immediately shows that the lateral spread of the dye will involve an uncertainty in the radial position. The lateral spread is greater at the more turbulent parts of the cycle. On the average, the lateral spread appears to depend little upon downstream distance. From measurement of projected photographs at the two phase angles of the experiments average lateral spreads of 0·44 and 0·24 radii at $\omega t = \frac{1}{2}\pi$ and $\omega t = 0$ were adopted. It follows that a dye patch seen in plan view to have a position r/a may actually be situated anywhere between r/a and $(r^2/a^2 + 0{\cdot}44^2)^{\frac{1}{2}}$, at $\omega t = \frac{1}{2}\pi$. Points will be plotted therefore at a radial position at the mean of these two values with an uncertainty of half their difference.

When $\omega t = \frac{1}{2}\pi$, figure 7, there appears to be no significant variation of drift distance with x over most of the range of x shown for $r/a < 0{\cdot}8$. For these points the asymptotic values were taken as the mean of the drift distances at large x values. One or two points in each r/a range were omitted as indicated in the figure by the extent of the horizontal lines. In finding the mean, the values were weighted according to the number of measurements involved in determining the

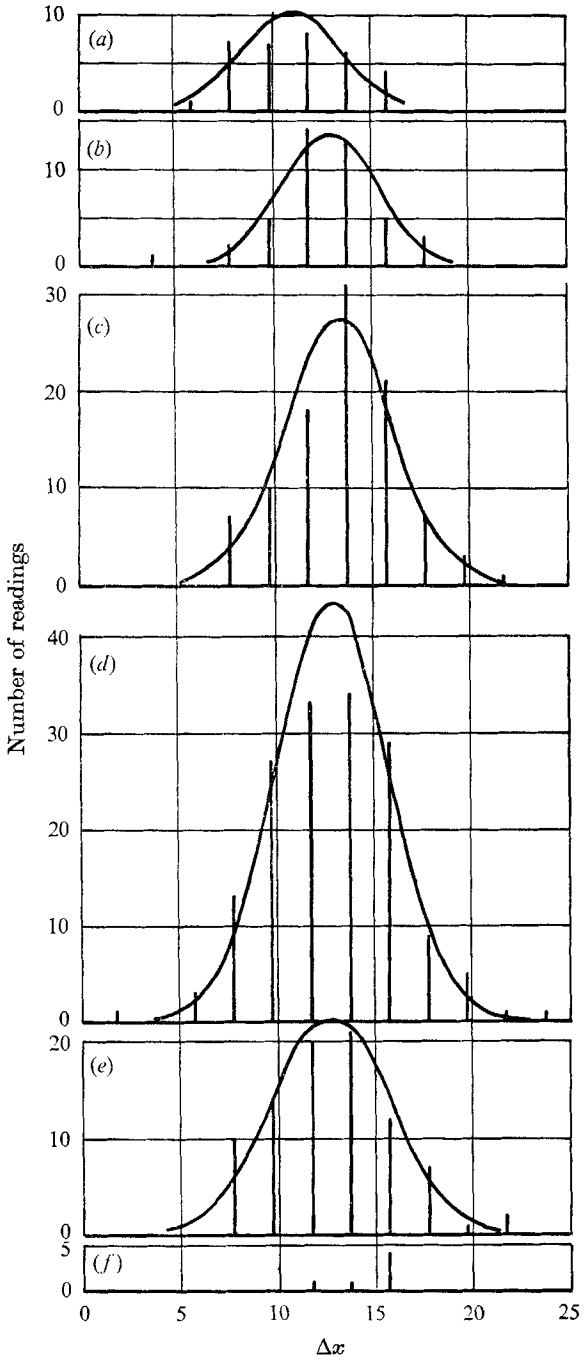

FIGURE 6. Distribution at the drift distance Δx in one camera framing interval ($\frac{1}{24}$ s) for $\omega t = \frac{1}{2}\pi$, $0 \leqslant r/a < 0{\cdot}2$, and a range of distances x downstream of the generating wire. Vertical lines indicate measurements, and the curves Gaussian distributions with the same mean value and standard deviation. The scale of Δx is measured on the projected image. (*a*) $0{\cdot}5 \leqslant x < 2{\cdot}5$ cm; (*b*) $2{\cdot}5 \leqslant x < 4{\cdot}5$; (*c*) $4{\cdot}5 \leqslant x < 6{\cdot}5$; (*d*) $6{\cdot}5 \leqslant x < 8{\cdot}5$; (*e*) $8{\cdot}5 \leqslant x < 10{\cdot}5$; (*f*) $10{\cdot}5 \leqslant x < 12$.

values. The similarly weighted standard deviation was also found. The limits of the standard deviations are shown in figure 7. When r/a is greater than 0·8, a different behaviour is observed. The curves drawn in this radial range in figure 7 indicate rough limits of possible variation of the asymptotic value. The asymptotic value is roughly equal to the value obtained close to the wire. It was

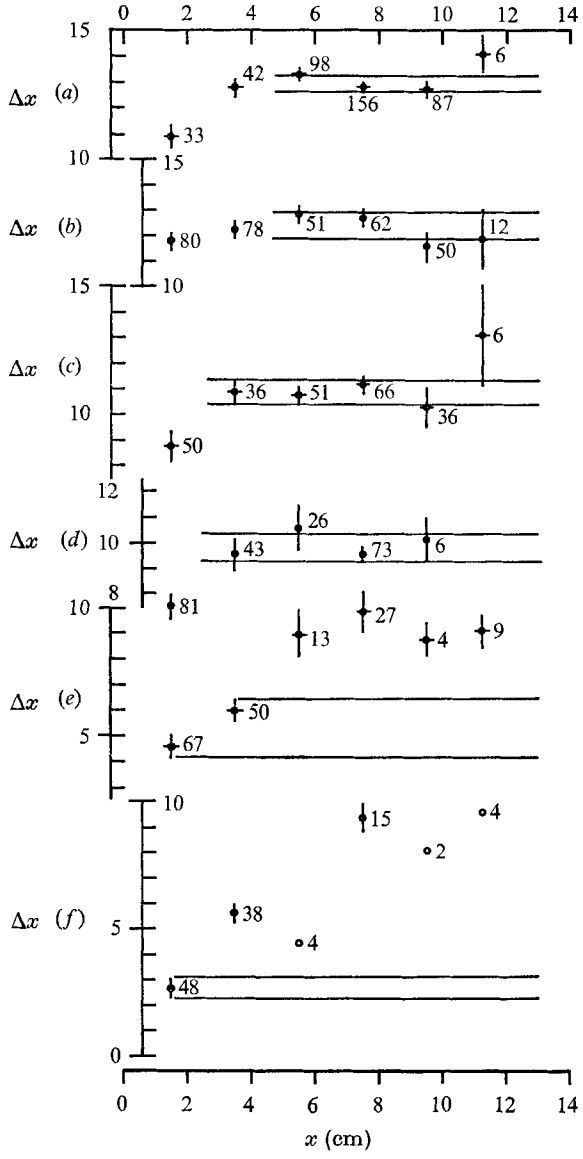

FIGURE 7. Drift distance as a function of distance downstream of the wire for $\omega t = \frac{1}{2}\pi$. Vertical lines through the points indicate the error of the mean value plotted. Numbers indicate the total number of measurements used to define the point. Horizontal lines define the standard deviation of the weighted mean of the derived drift distance. (*a*) $0 \leqslant r/a < 0{\cdot}2$; (*b*) $0{\cdot}2 \leqslant r/a < 0{\cdot}4$; (*c*) $0{\cdot}4 \leqslant r/a < 0{\cdot}6$; (*d*) $0{\cdot}6 \leqslant r/a < 0{\cdot}8$; (*e*) $0{\cdot}8 \leqslant r/a < 0{\cdot}9$; (*f*) $0{\cdot}9 \leqslant r/a < 0{\cdot}95$.

found that this produced the correct velocity in a steady turbulent flow where the same sort of discrepancy was observed. The convected dye indicates different velocities close to and far from the wire. Close to the wire one sees folds of dye drifting along the wall. Far from the wire these folds become too nearly parallel to the tube axis to measure their displacement. What does become visible and

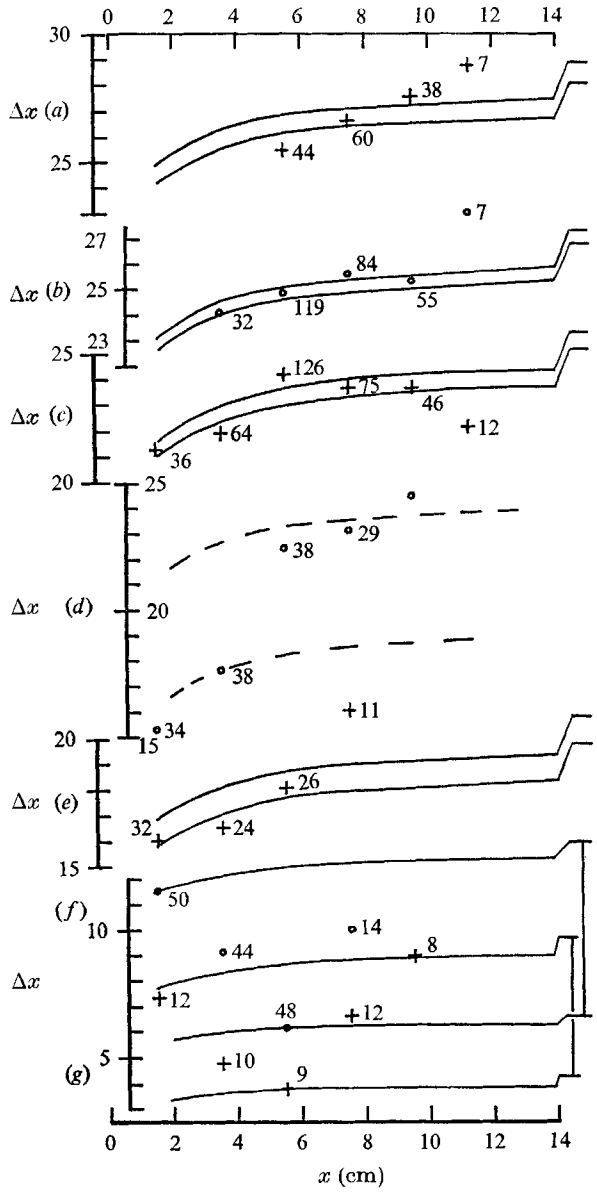

FIGURE 8. Drift distance as a function of distance downstream of the wire for $\omega t = 0$. Curves correspond to a variation of velocity error as $x^{-\frac{1}{2}}$. Separation of curves is twice the weighted standard deviation of the points from the mean of the pair of curves, except for $0{\cdot}6 \leqslant r/a < 0{\cdot}7$ and $r/a \geqslant 0{\cdot}8$. (*a*) $0 \leqslant r/a < 0{\cdot}2$; (*b*) $0{\cdot}2 \leqslant r/a < 0{\cdot}4$; (*c*) $0{\cdot}4 \leqslant r/a < 0{\cdot}6$; (*d*) $0{\cdot}6 \leqslant r/a < 0{\cdot}7$; (*e*) $0{\cdot}7 \leqslant r/a < 0{\cdot}8$; (*f*) $0{\cdot}8 \leqslant r/a < 0{\cdot}9$; (*g*) $0{\cdot}9 \leqslant r/a < 0{\cdot}95$.

what is measured are contortions due to turbulent eddies which are travelling nearer to the axis at higher speed. This is more clearly demonstrated when one views particles which have drifted along the bottom of the tube. These are in apparent laminar motion for most of the time, but are occasionally stirred up by a much more rapidly moving disturbance which can be seen to be travelling through the particles. The particles reverted to their laminar motion after the disturbance had passed. The higher velocity indicated in figure 7 at $r/a > 0{\cdot}8$ is that corresponding to $0{\cdot}6 \leqslant r/a < 0{\cdot}8$, which substantiates this explanation.

The measurements at $\omega t = 0$ were more difficult than those at $\omega t = \frac{1}{2}\pi$, because sufficiently clearly defined patches of dye had to be searched for. Even so, the standard deviation is little larger in the centre of the tube where the radial gradient of velocity is small. The velocity deficit does not have as smooth a variation with downstream distance. From casual observation of figure 8 it may be supposed that the asymptotic value was reached as soon as in the turbulent flow at $\omega t = \frac{1}{2}\pi$. Curves varying as $x^{-\frac{1}{2}}$ obtained from laminar flow investigations may also be fitted to the points as has been done in figure 8. These curves again show the limits of the weighted standard deviations of all points from the mean curve. The elevated asymptotic levels, indicated at the right of the figure, give a sectional mean velocity which agrees with the directly measured value. In laminar flow the asymptotic value is only achieved very far downstream.

It will be shown that there are large radial gradients of velocity at $r/a > 0{\cdot}6$. For $0{\cdot}6 \leqslant r/a < 0{\cdot}7$ the distribution of drift measurements (cf. figure 6 for $\omega t = \frac{1}{2}\pi$) was widely scattered; also, most of the points lay near 0·6 and 0·7, and very few in between. Curves for the adjacent ranges are drawn in figure 8 on the points for $0{\cdot}6 \leqslant r/a < 0{\cdot}7$, and it is seen that the points generally fall on one curve or the other. No conclusion about the flow speed was drawn from this range of points.

Close to the wall the behaviour is different from steady turbulent flow and from the $\omega t = \frac{1}{2}\pi$ results. The points in this range ($r/a > 0{\cdot}8$) were used simply to define a range of velocities within which it seemed likely that the true velocity fell. In this experiment, where there exists an independently determined mean velocity with which the velocity profile must conform, the indeterminacy is not as bad as figure 8 would at first appear to suggest.

We may conclude that the method of velocity measurement is limited in application. The convection speed of particles of dye in turbulent flow no doubt gives the flow speed at that instant. Particles of dye must be visible and drift measurable in all conditions of the flow to obtain a true indication of mean velocity. When there are gradients of velocity, the eddy size responsible for producing the dye patches must be smaller than the scale of the mean velocity changes, or erroneous convection speeds will result.

7. Presentation of results and discussion

7.1. *The mean flow velocity distribution*

Measurements were first made on steady turbulent flow to test the method. Several published velocity profiles exist for steady flow. Those of Nikuradse, as

reported by Schlichting (1955) at $Re = 4000$ and Laufer (1954) at $Re = 5 \times 10^4$, are in agreement to within 1 % for $r/a \leqslant 0{\cdot}7$. The measurements of Sandborn (1955) lie within 2–3 % below these values. As Reynolds number decreases the velocity normalized with the centre-line velocity is lower at $r/a > 0{\cdot}7$. Senecal & Rothfus (1953) have made measurements over the transition range of Reynolds number, in particular at $Re = 3464$ and 4085. Similar measurements, agreeing closely with Senecal & Rothfus, were reported by Patel & Head (1969). The mean profile used here was compiled from the published results. The ratio of mean to centre-line velocity was found to be 0·77, which lies satisfactorily between the values of 0·73, found by Senecal & Rothfus and Patel & Head, and the value of 0·79 due to Nikuradse. The mean velocity was determined to 1 % by measuring the volume flow from the outlet. The results are presented as the oscillating component of the flow by subtracting the mean flow profile from the measured profile and are shown in figures 9 and 10. The laminar oscillating profiles from figure 4 are included for comparison. The limits are the weighted standard deviations from figures 7 and 8 and the range of possible r/a values. It is estimated that the steady-flow profile, which is subtracted to obtain the oscillating profiles, has an error of 2 % of the mean velocity. There is thus an additional uncertainty of $\pm 0{\cdot}2\,\mathrm{cm\,s^{-1}}$ in figures 9 and 10.

7.2. *A physical description of the flow*

The velocity profile, as in the case of laminar flow discussed in § 2, is determined by diffusion of vorticity, and by the fact that the cross-sectional mean velocity is equal to the piston velocity ($-5{\cdot}1\,\mathrm{cm\,s^{-1}}$ in figure 9 and zero in figure 10). Unlike pulsations in laminar flow, the results are dependent on the mean flow and cannot be considered apart from it. The Reynolds number of this experiment lies in the transition range; consequently the effect of pulsation on the turbulent structure is very noticeable in the appearance of the flow (see figures 3(*a*)–(*h*), plates 2–5). At any high Reynolds number the structure of turbulence changes during the cycle of pulsation. The turbulence intensity diminishes during acceleration, a phenomenon known as laminarization, and in decelerating flow the turbulence intensity increases.

As a result, there is a change in the velocity profile. At high enough Reynolds number the turbulence is sufficiently intense in the accelerating phase for this effect to be small except close to the wall. In the transitional range of these experiments, on the other hand, the flow appears almost laminar for nearly half the cycle. The velocity profile is still essentially that corresponding to turbulent flow with a relatively small effect of laminarization. This is because the characteristic time for vorticity diffusion is much larger in laminar flow than it is in turbulent flow. The ratio of this time to a period T is a measure of the amount the mean profile can change in one period when the turbulence appears or disappears. This ratio $a^2/\nu T \simeq 30$ in this experiment, whereas in the centre of the tube, $r/a \leqslant 0{\cdot}8$, the eddy viscosity ϵ is about 10 times the kinematic viscosity and $a^2/\epsilon T \simeq 3$. Turbulent diffusion being ten times more effective than molecular

diffusion over most of the flow the effective mean profile will be the turbulent one. The effect of laminarization will have to be considered, in particular close to the wall.

The eddy viscosity is a function of Reynolds number, and so will change as the flow speed changes. This effect is not strong and is completely masked by the much stronger effect of acceleration. The detailed effect of acceleration on the turbulence is not known. We define the steady profile which must be subtracted from the measured profile to produce the oscillating component as the profile of the flow at the mean speed. It will be shown that the changes of eddy viscosity through the cycle do not produce a strong effect when there is an appreciable mean flow. The problem of oscillating flow, with zero mean and large enough amplitude to be turbulent for part of the cycle, is more complicated, and is a different problem.

It may be that such a condition of mixed flow cannot be achieved. The production of turbulence in the decelerating phase is likely to be delayed to such a high Reynolds number that once started it will not again go laminar. In the present apparatus, with or without pulsations, the time which elapsed between starting and turbulence being observed was the time for convection from the entry to the point of observation. In a smooth tube far from the piston and from the other end, the flow will not become turbulent until very high Reynolds numbers, and once turbulent it will be intensely so.

7.3. *The form of the oscillating velocity profile at* $\omega t = \frac{1}{2}\pi$

We turn now to explain the form of the curves at the two-phase angles of this experiment, and to extrapolate the findings to higher Reynolds numbers and different frequencies. Consider the phase angle $\omega t = \frac{1}{2}\pi$ and the part of the profile in the range $0 < r/a < 0{\cdot}6$, where we see from figure 9 that the velocity is essentially constant as in laminar oscillating flow. The central flat part of the profile remains, because the profile has not had time to change. The kinematic viscosity ν has been replaced by the eddy viscosity ϵ, and thus diffusion is accelerated. The reasoning above shows that, even where $\epsilon = 10\nu$, which is only the case for the central half of the tube, the characteristic diffusion time is three periods. The flow has been strongly turbulent for only about a quarter of a period at $\omega t = \frac{1}{2}\pi$; thus, the change will be small. The effective value of Ω is reduced from its laminar value, but it is no longer independent of radial distance, since ϵ is a function of r. The trend in turbulent flow will be the same as in laminar flow namely that at small values of Ω the flow is effectively steady at each instant. In figure 9, therefore, a profile is drawn which varies as a turbulent profile near to the wall: $u \propto y^{\frac{1}{7}}$, y being distance from the wall. The curve is flattened in the centre of the tube to produce the correct sectional mean value of $-5{\cdot}1$ cm/s. One expects that a flat central portion will persist in turbulent flow unless, as at high Reynolds number, the eddy viscosity is very much greater than the molecular viscosity. The measured values lie close to this suggested profile. If they are reduced by 0·2 cm/s, the estimated error of the mean profile, excellent agreement is obtained. The discrepancy could, on the other hand, be the

remnants of the effects of laminarization, which, as we shall see, elevates the curve in the centre and reduces it in the region of $r/a = 0{\cdot}9$.

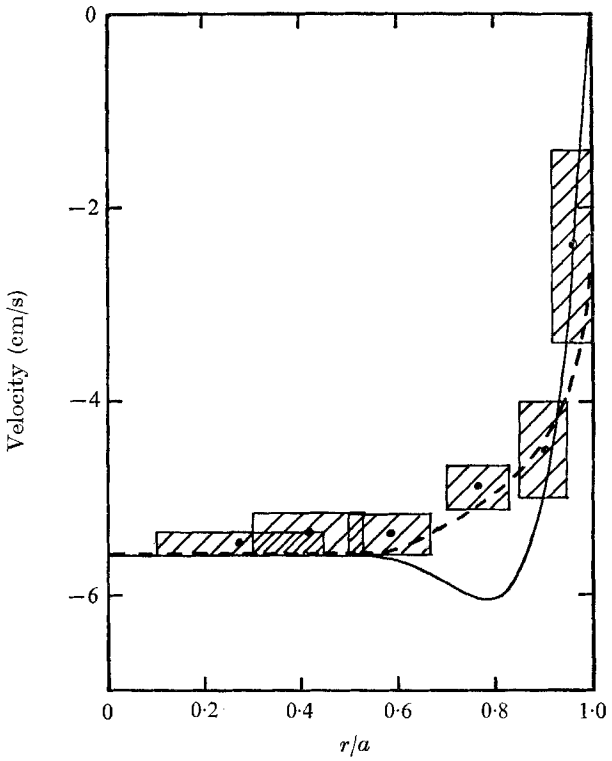

FIGURE 9. Oscillating component of pulsating flow at $Re = 3770$ when the piston is advancing against the mean flow at its maximum speed ($\omega t = \frac{1}{2}\pi$). Laminar oscillating profile for same value of $\Omega = a\sqrt{(\omega/\nu)} = 14{\cdot}4$, —; curve having mean value equal to piston speed and a turbulent profile $u \propto y^{\frac{1}{8}}$ near the wall, – – –.

7.4. *Extrapolation to higher Reynolds numbers and different frequencies*

At higher Reynolds numbers one would expect there to be no flat central portion; the turbulent profile ($u \propto y^{1/n}$) will extend up to the axis. The increase in diffusivity attending the increase in turbulence will ensure that the value of Ω is low, unless the real frequency is very large. The effects of laminarization decrease as Reynolds number increases and are confined to a wall layer. The value of the eddy viscosity must be computed to determine the expected performance. Brinkworth & Smith (1969) give the equation

$$\epsilon^{\dagger} = \frac{\epsilon}{u_\tau a} = \frac{K}{6}\left(1-\frac{r^2}{a^2}\right)\left(1+2\frac{r^2}{a^2}\right), \tag{12}$$

where $u_\tau = \sqrt{(\tau_0/\rho)}$ is the friction velocity, and K is 0·4 and independent of

Reynolds number at high Reynolds number. Reference to Schlichting (1955) shows that

$$\frac{\epsilon}{\nu} = \frac{\epsilon^+}{2}\sqrt{(f/8)}\, Re,$$

where f is the friction factor. In the transition range of Reynolds number, where the Brinkworth & Smith equation for e^+ is inaccurate, the eddy viscosity is obtained from the slope of the velocity profile. The relation,

$$\epsilon^+ = -\frac{(r/a)\, u_\tau}{du/d(r/a)}, \tag{13}$$

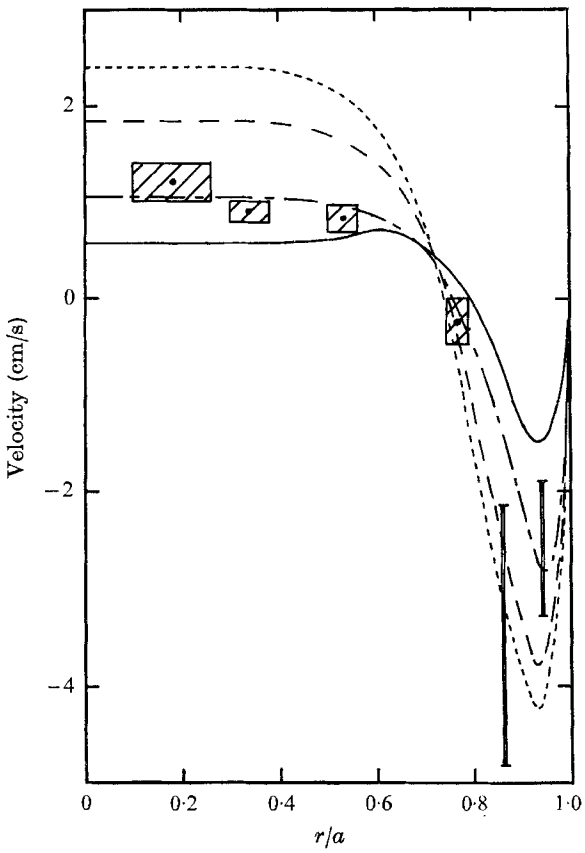

FIGURE 10. Oscillating component of pulsating flow at $Re = 3770$, when the piston is fully retracted ($\omega t = 0$). Laminar oscillating profile for same value of $\Omega = a\sqrt{(\omega/\nu)} = 14{\cdot}4$, —. Calculated for laminar period of $\frac{3}{4}\pi$, – – – –, $\frac{1}{2}\pi$, ———, and $\frac{1}{4}\pi$, — — —.

may be obtained from the equation for the Reynolds stress,

$$\overline{uv} = \nu\frac{du}{dr} + \frac{r}{a}u_\tau^2, \tag{14}$$

which is derived by Laufer (1954).

The form of the oscillating component is determined by $a\sqrt{(\omega/\epsilon)}$. At high Reynolds numbers, where the value of this quantity is low except very close to the wall, we expect the form of the oscillating profile to be $u \propto y^{1/n}$. The effects of

laminarization may be expected to be small, and will be reflected in the changing value of n through the cycle of oscillation. Reference to the changing form of the mean velocity profile with Reynolds number, as determined by Nikuradse and reproduced by Schlichting (1955), shows that a change of an order of magnitude in the Reynolds number only changes the mean velocity by 3 or 4 % at most except very close to the wall. The effect of changing turbulence intensity during a cycle of oscillation will thus have little effect on the oscillating component of the velocity. At low Reynolds numbers as here, the degree of laminarization has a large effect because the turbulence almost disappears for part of the cycle.

7.5. *The form of the oscillating component of the velocity profile at* $\omega t = 0$

The pulsating flow profile at $\omega t = 0$ is strongly dependent upon its location at the end of a period of turbulence free flow. The profile at this phase has been investigated by laminar flow theory. Parallel work on the numerical solution of the equations for axisymmetric incompressible flow was easily adapted to study this problem. Details are omitted here but will be published later. The equations of motion are solved by means of the vorticity and continuity equation, which, for parallel flow, are

$$\frac{\partial \eta}{\partial t} = \frac{1}{R}\left(\frac{\partial^2 \eta}{\partial r^2} + \frac{1}{r}\frac{\partial \eta}{\partial r} - \frac{\eta}{r^2}\right), \tag{15}$$

which is obtained by differentiating (1), and

$$\eta = \frac{1}{r}\left(\frac{\partial^2 \psi}{\partial r^2} - \frac{1}{r}\frac{\partial \psi}{\partial r}\right), \tag{16}$$

where η is the vorticity $= -\partial u/\partial r$, ψ is the stream function,

$$u = -\frac{1}{r}\frac{\partial \psi}{\partial r},$$

and R is the Reynolds number, if the tube diameter and a velocity are used to non-dimensionalize the equation. If the period of oscillation and the radius are used to non-dimensionalize, R is $a^2/\nu T$ which is related to Ω. The solution of these equations has been shown to reproduce the laminar pulsating flow profiles of § 2 to within 1 %. The equations are written in terms of central finite differences, and, with the appropriate boundary conditions, are solved on a digital computer.

The effect of laminarization can be studied by means of this computer programme if the flow reverts completely to laminar motion. At the end of the turbulent phase of the motion, we predict that the oscillating profile will be a mean turbulent flow profile ($u/U \propto (y/a)^{1/n}$) near the wall and flat in the centre of the pipe. The mean velocity is known. It was assumed that $n = 6$, and that the central flat profile extends to $r/a = 0{\cdot}5$. The initial velocity profile is the mean turbulent profile plus the turbulent oscillating profile. Given sufficient time the computed profiles will be those of Poiseuille flow plus the laminar oscillating profile. The profiles were calculated at $\omega t = 0$ after starting as described above at $\omega t = -\frac{3}{4}\pi$, $-\frac{1}{2}\pi$ and $-\frac{1}{4}\pi$. The resulting oscillating component obtained by subtracting the mean turbulent profile are included in figure 10. Obviously, assuming that the

flow is laminar for $\frac{3}{8}$ of the period overestimates the effect of laminarization. The almost laminar appearance of the dyed flow is deceptive. The apparently slight vestiges of turbulence are evidently sufficient to considerably arrest the development of a laminar flow profile. We can only conclude that the effect of laminarization is closely equivalent, at $\omega t = 0$, to a fully laminar flow for the interval of $\frac{1}{4}\pi$ immediately preceding $\omega t = 0$. This effect is only expected to be strong in the transition range of the Reynolds numbers.

8. Conclusions

The oscillating component of pulsating turbulent flow has been defined as the velocity profile obtained by subtracting the profile corresponding to steady turbulent flow at the mean velocity from the profile measured at any instant of the motion. The profile changes because the turbulent structure of the flow changes; acceleration reducing the turbulent intensity, deceleration increasing it. As in the case of laminar flow, the profile also changes because vorticity creation at the wall is constantly changing and vorticity diffuses across the flow.

The Reynolds number of this experiment lies in the transition range, so that during the accelerating phase the turbulence almost disappears. Experiments were made at one non-dimensional frequency $\Omega = a\sqrt{(\omega/\nu)} = 14{\cdot}4$. In laminar flow at this frequency the velocity profile possesses a central plateau extending to half the tube radius. This is found to be unaltered in extent by the turbulence at this Reynolds number. During the turbulent phase its magnitude is almost the same. Closer to the wall the oscillating profile is well represented by $u/U \propto (y/a)^{1/n}$ in the turbulent phase. In the accelerating phase laminarization is well advanced at this Reynolds number, and the profile depends strongly on the extent of laminar flow. The effect is shown to correspond to complete laminarization for one-eighth of the period in these experiments.

At higher Reynolds numbers the flow will be turbulent for the whole cycle. Small laminarization effects through the change in the exponent n are expected. The central part of the velocity profile is expected to become more rounded following the mean turbulent flow type.

REFERENCES

Baker, D. J. 1966 A technique for the precise measurement of small fluid velocities. *J. Fluid Mech.* **26**, 573.

Brinkworth, B. J. & Smith, P. C. 1969 Velocity distribution in the core of a turbulent pipe flow. *Chem. Eng. Sci.* **24**, 787.

Combs, G. D. 1964 A stability study for pulsating flow in rigid tubes. Ph.D. Thesis, University of Arkansas.

Davis, W. & Fox, R. W. 1967 An evaluation of the hydrogen bubble technique for the quantitative determination of fluid velocities within clear tubes. *J. Basic Engng* **89**, 771.

Laufer, J. 1954 The structure of turbulence in fully developed pipe flow. *NACA Rep.* no. 1174.

Linford, R. G. & Ryan, N. W. 1965 Pulsatile flow in rigid tubes. *J. Appl. Physiol.* **20**, 1078.

Patel, V. C. & Head, M. R. 1969 Some observations on skin friction and velocity profiles in fully developed pipe and channel flows. *J. Fluid Mech.* **38**, 181.

SANDBORN, V. A. 1955 Experimental evaluation of the momentum terms in turbulent pipe flow. *NACA Tech. Note* no. 3266.

SCHLICHTING, H. 1955 *Boundary Layer Theory* (1st English edn). Oxford: Pergamon.

SENECAL, V. E. & ROTHFUS, R. R. 1953 Transition flow in smooth tubes. *Chem. Engng Prog.* **49**, 533.

SEXL, T. 1930 Über den von E. G. Richardson entdeckten 'Annulareffekt'. *Z. Phys.* **61** 349.

SZYMANSKI, F. 1930 Quelques solutions exactes des equations de l'hydrodynamique de fluide visqueux dans le cas d'un tube cylindrique. *Proc. 3rd Int. Congr. Appl. Mech.* **1**, 249.

UCHIDA, S. 1956 The pulsating viscous flow superposed on the steady motion of incompressible fluid in a circular pipe. *Z.A.M.P.* **7**, 403.

WOMERSLEY, J. R. 1955 Oscillatory motion of a viscous fluid in a thin walled elastic tube. *Phil. Mag.* **46**, 199.

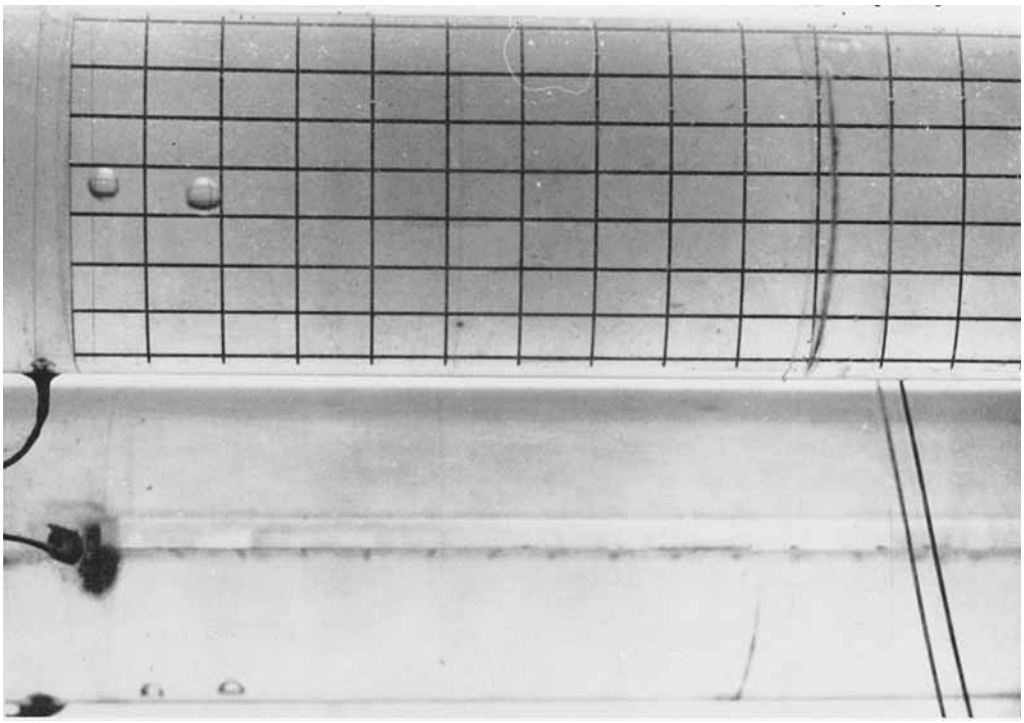

FIGURE 1. Calibration.

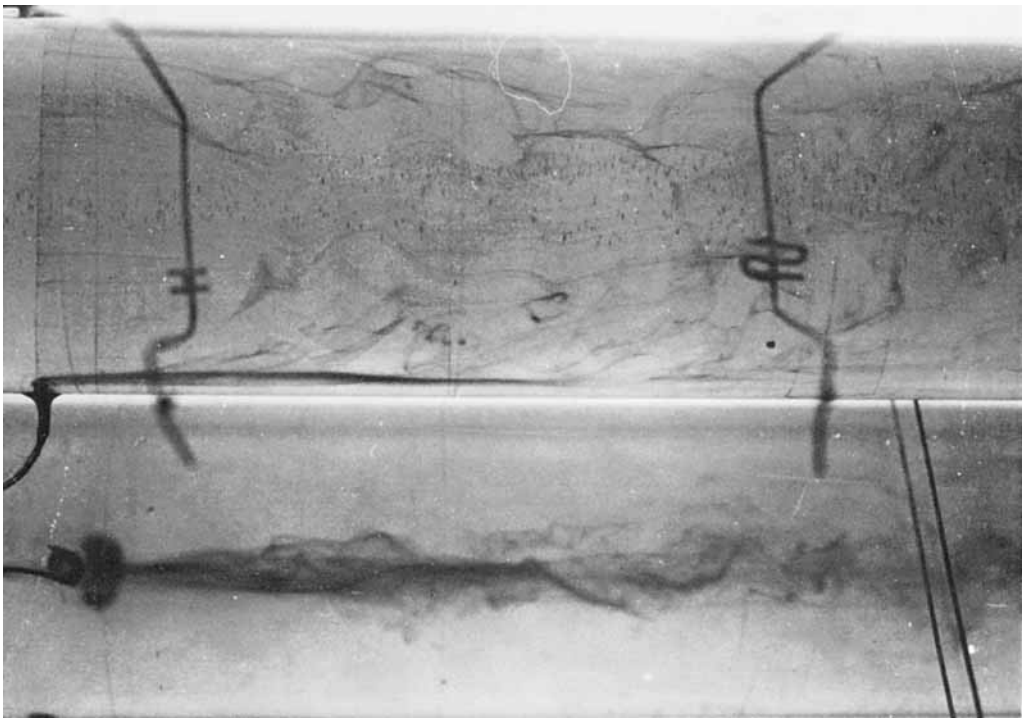

FIGURE 2. Steady turbulent flow.

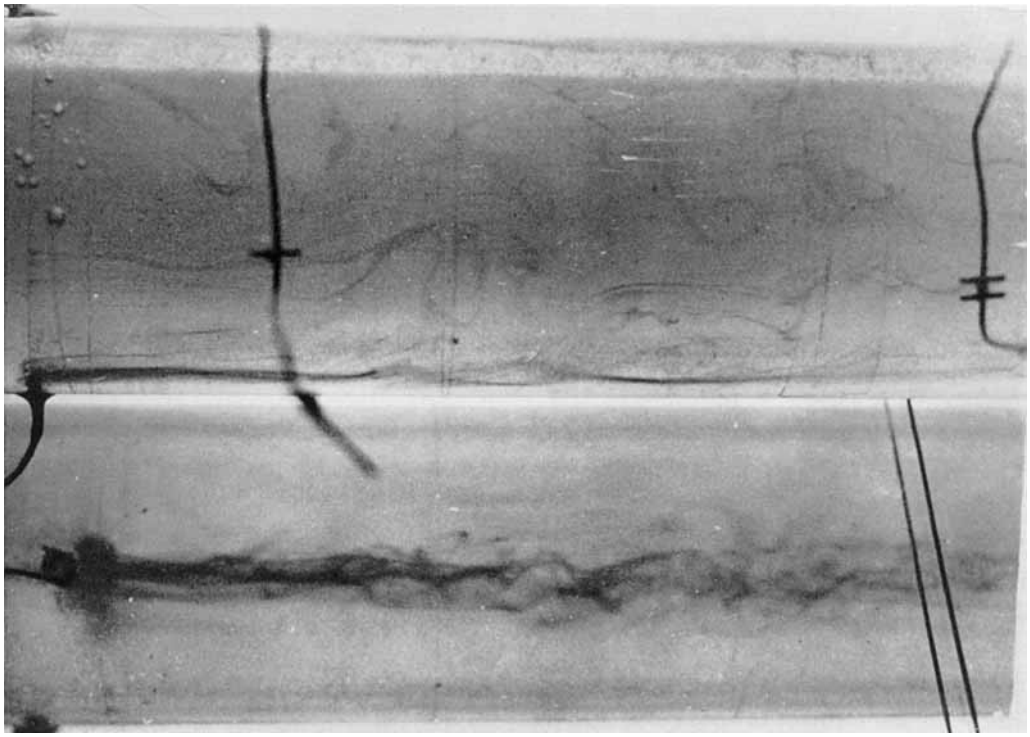

(*a*)

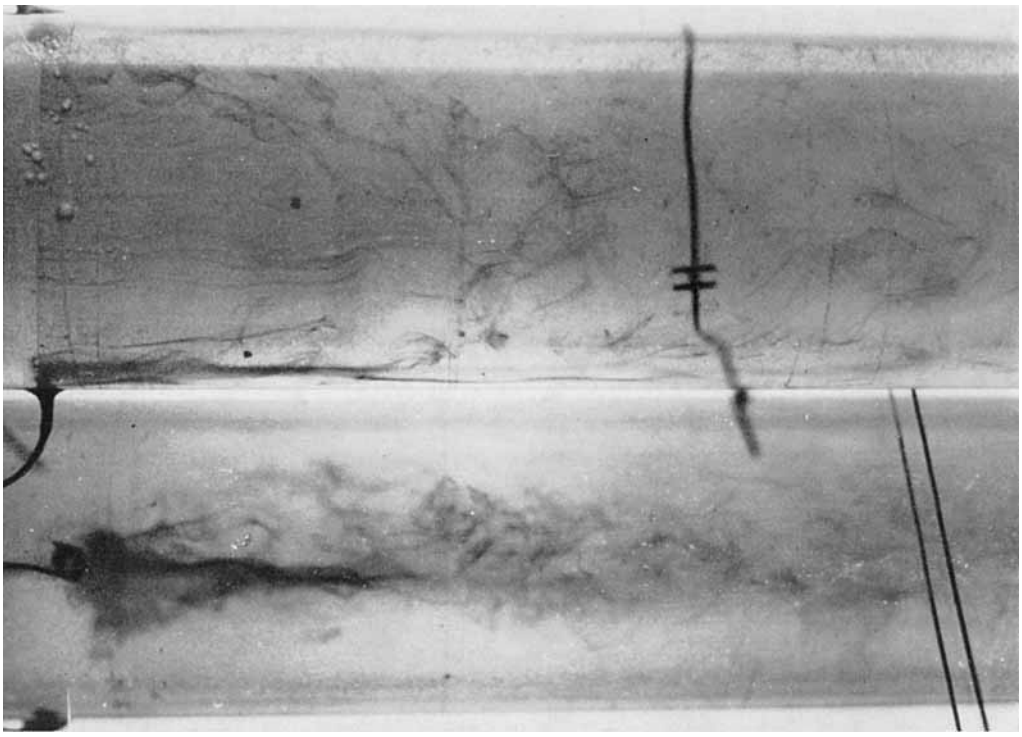

(*b*)

FIGURE 3. Pulsating flow (*a*) $\omega t = 0$ (piston fully retracted), (*b*) $\omega t \simeq \frac{1}{4}\pi$ (piston moving against mean flow), (*c*) $\omega t \simeq \frac{1}{2}\pi$, (*d*) $\frac{3}{4}\pi$, (*e*) π, (*f*) $\frac{5}{4}\pi$, (*g*) $\frac{3}{2}\pi$, (*h*) $\frac{7}{4}\pi$.

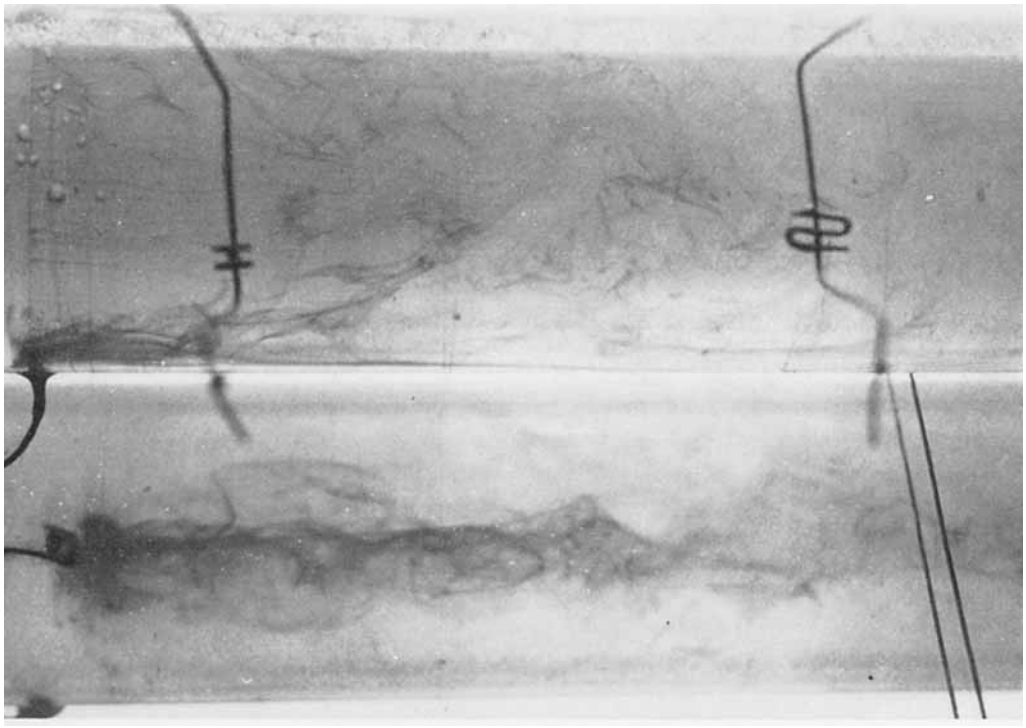

(*c*)

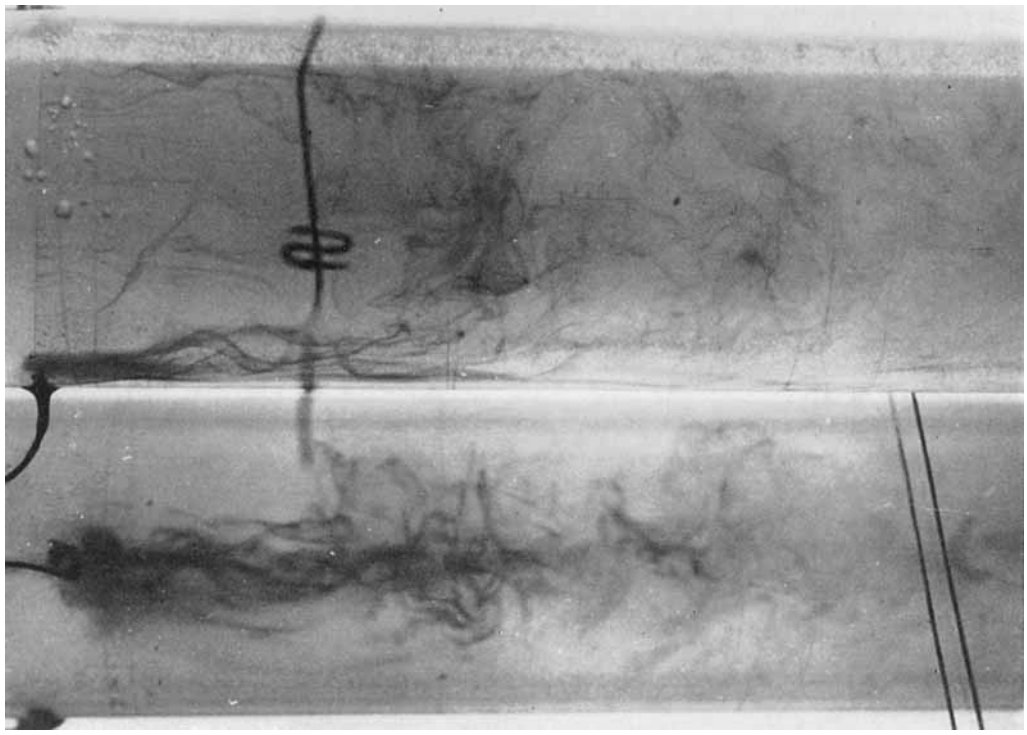

(*d*)

FIGURE 3. See plate 2 for legend.

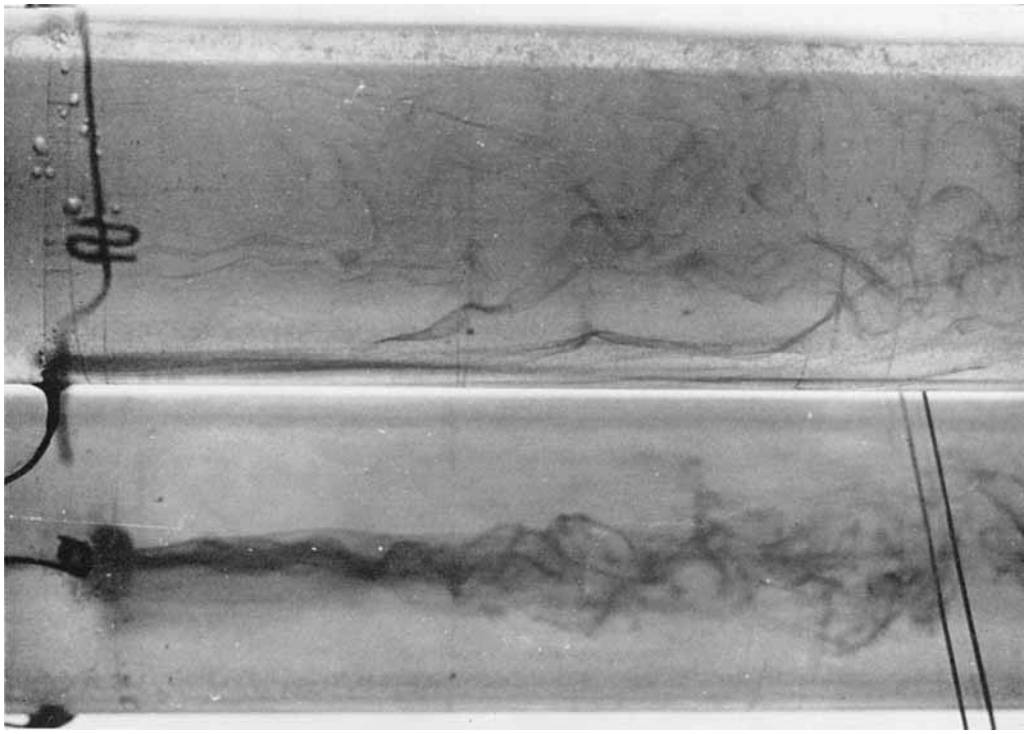

(*e*)

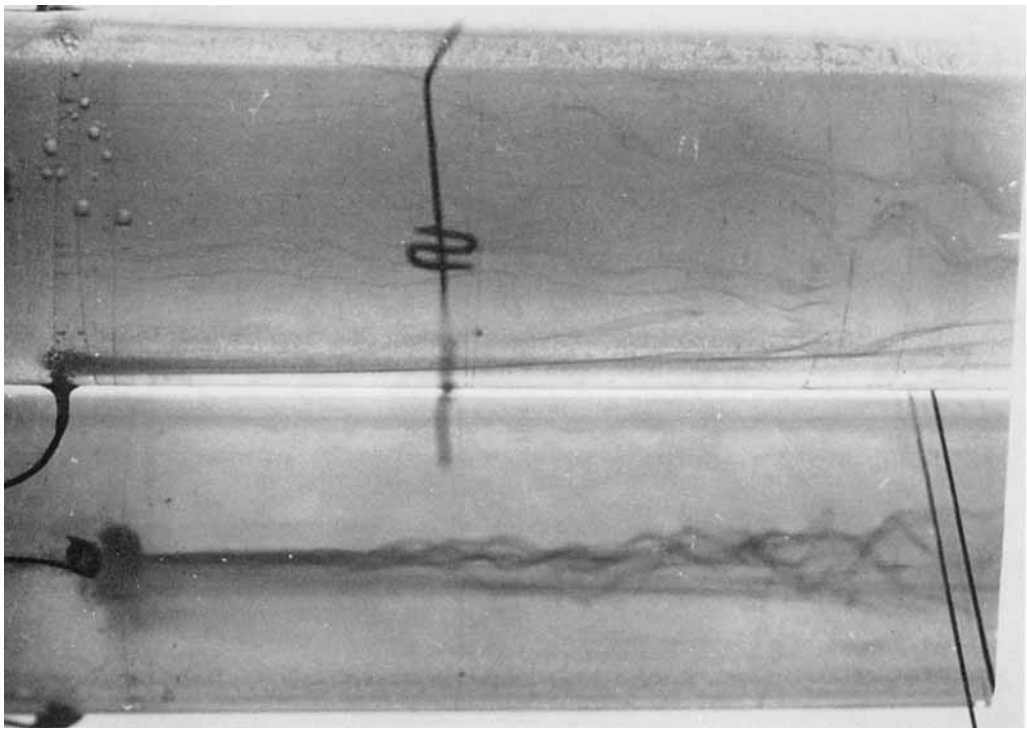

(*f*)

FIGURE 3. See plate 2 for legend.

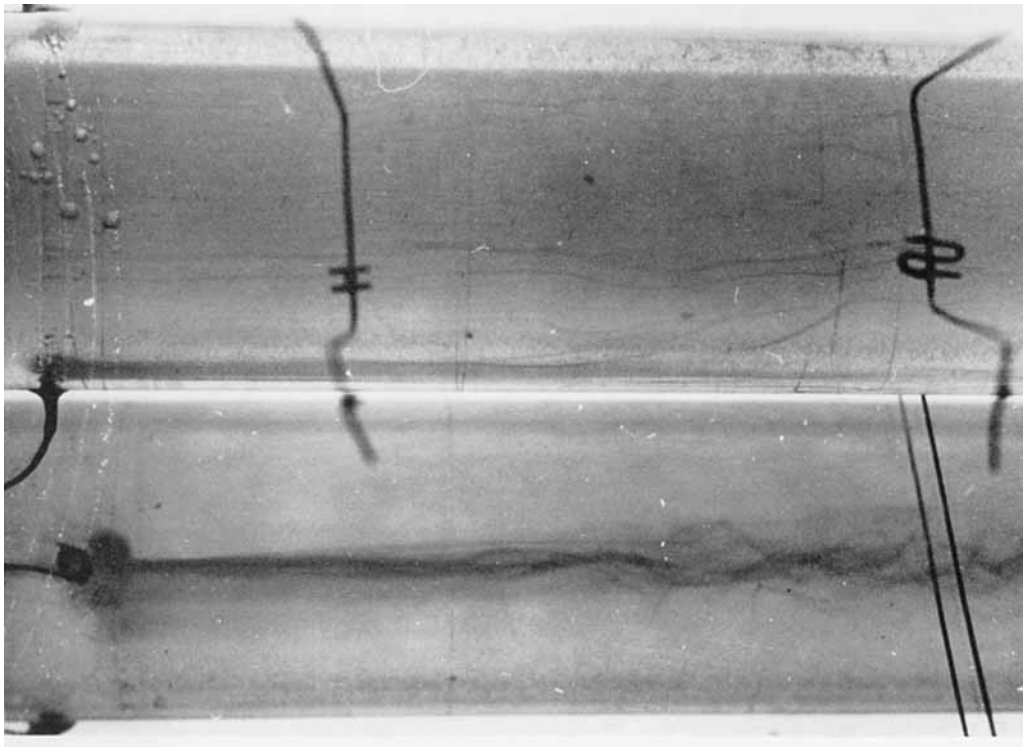

(*g*)

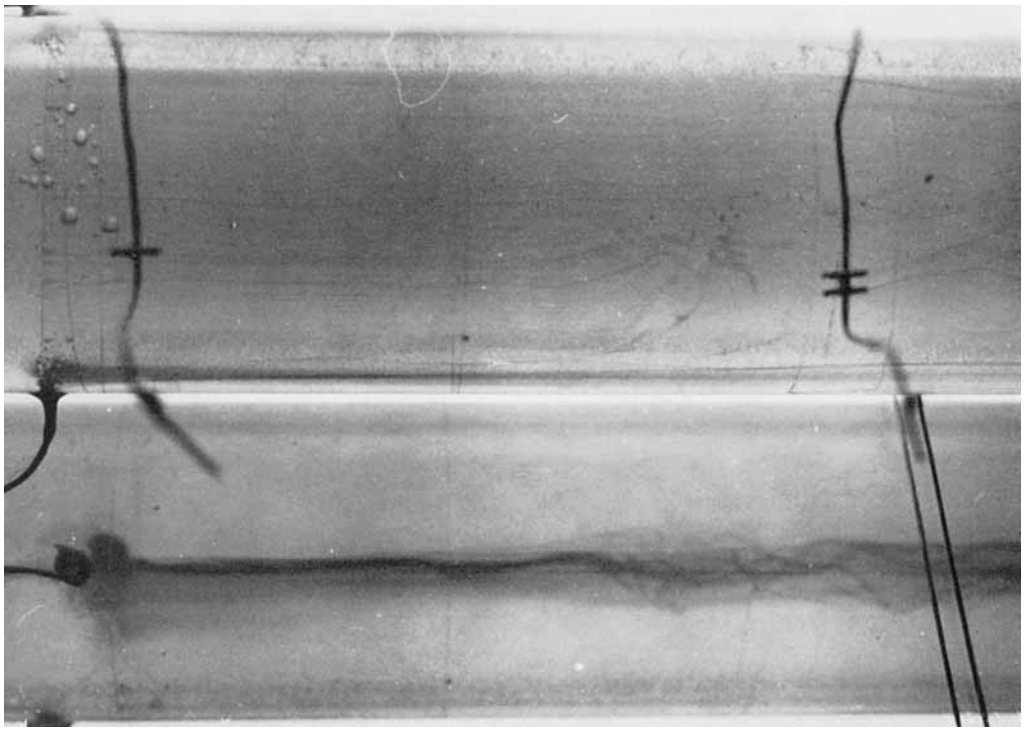

(*h*)

FIGURE 3. See plate 2 for legend.